

Neuronal Nitric Oxide Synthase Protects Against Myocardial Infarction–Induced Ventricular Arrhythmia and Mortality in Mice

Dylan E. Burger, PhD*; Xiangru Lu, MD*; Ming Lei, MD; Fu-Li Xiang, MD; Lamis Hammoud, PhD; Mao Jiang, PhD; Hao Wang, MD, PhD; Douglas L. Jones, PhD; Stephen M. Sims, PhD; Qingping Feng, MD, PhD

Background—Neuronal nitric oxide synthase (nNOS) is expressed in cardiomyocytes and plays a role in regulating cardiac function and Ca^{2+} homeostasis. However, the role of nNOS in cardiac electrophysiology after myocardial infarction (MI) is unclear. We hypothesized that nNOS deficiency increases ventricular arrhythmia and mortality after MI.

Methods and Results—MI was induced in wild-type (WT) or nNOS^{-/-} mice by ligation of the left coronary artery. Thirty-day mortality was significantly higher in nNOS^{-/-} compared with WT mice. Additionally, nNOS^{-/-} mice had impaired cardiac function 2 days after MI. Telemetric ECG monitoring showed that compared with WT, nNOS^{-/-} mice had significantly more ventricular arrhythmias and were more likely to develop ventricular fibrillation after MI. Treatment with the L-type Ca^{2+} channel blocker verapamil reduced the incidence of arrhythmia and ventricular fibrillation in nNOS^{-/-} mice after MI. To assess the role of nNOS in Ca^{2+} handling, patch-clamp and Ca^{2+} fluorescence techniques were used. Ca^{2+} transients and L-type Ca^{2+} currents were higher in nNOS^{-/-} compared with WT cardiomyocytes. Additionally, nNOS^{-/-} cardiomyocytes exhibited significantly higher systolic and diastolic Ca^{2+} over a range of pacing frequencies. Treatment with the NO donor S-nitroso N-acetyl-penicillamine decreased Ca^{2+} transients and L-type Ca^{2+} current in both nNOS^{-/-} and WT cardiomyocytes. Furthermore, S-nitrosylation of Ca^{2+} handling proteins was significantly decreased in nNOS^{-/-} myocardium after MI.

Conclusions—Deficiency in nNOS increases ventricular arrhythmia and mortality after MI in mice. The antiarrhythmic effect of nNOS involves inhibition of L-type Ca^{2+} channel activity and regulation of Ca^{2+} handling proteins via S-nitrosylation. (*Circulation*. 2009;120:1345-1354.)

Key Words: arrhythmia ■ calcium ■ myocardial infarction ■ nitric oxide ■ nitric oxide synthase

Neuronal nitric oxide (NO) synthase (nNOS) is a Ca^{2+} -dependent enzyme initially identified in the brain and implicated in neurotransmission.^{1,2} Along with endothelial nitric oxide synthase (eNOS) and inducible NOS, nNOS belongs to a class of enzymes that produce NO through the conversion of L-arginine to L-citrulline.³ More recently, it has been demonstrated that nNOS is expressed in cardiomyocytes and localized to the sarcoplasmic reticulum.⁴ Interestingly, nNOS has been shown to be physically associated with the ryanodine receptor Ca^{2+} release channel (RyR2) and SERCA2.^{5,6} Under conditions in which nNOS is overexpressed in cardiomyocytes, it also binds to the L-type Ca^{2+} channel.⁶ Given the close association between nNOS and the proteins that are important in the regulation of Ca^{2+} , it is not surprising that nNOS regulates intracellular Ca^{2+} ($[\text{Ca}^{2+}]_i$) levels in cardiomyocytes.^{6,7} Indeed, nNOS deletion is as-

ociated with increased Ca^{2+} transient amplitude and L-type Ca^{2+} currents ($I_{\text{Ca,L}}$), as well as reduced phospholamban phosphorylation and increased cardiomyocyte shortening.⁷⁻⁹ Additionally, nNOS-derived NO has been shown to inhibit myocardial responsiveness to β -adrenergic stimulation.^{8,10} Taken together, these observations indicate that nNOS plays an important physiological role in regulating Ca^{2+} cycling and cardiac function.¹¹

Clinical Perspective on p 1354

Studies have found that nNOS expression and nNOS-derived NO production are increased in human and rat hearts during heart failure.^{5,12} However, the role of nNOS in heart failure is still not fully understood. Initial studies by Bendall et al¹³ showed that rats with myocardial infarction (MI)-induced heart failure exhibit increased myocardial sensitivity

Received July 3, 2008; accepted July 2, 2009.

From the Departments of Physiology and Pharmacology (D.E.B., F.-L.X., L.H., M.J., D.L.J., S.M.S., Q.F.), Medicine (M.L., D.L.J., Q.F.), and Surgery (H.W.), University of Western Ontario, and Lawson Health Research Institute (X.L., H.W., D.L.J., Q.F.), London, Ontario, Canada.

*Drs Burger and Lu contributed equally to this work.

The online-only Data Supplement is available with this article at <http://circ.ahajournals.org/cgi/content/full/CIRCULATIONAHA.108.846402/DC1>. Correspondence to Dr Qingping Feng, Department of Physiology and Pharmacology, University of Western Ontario, London, Ontario, Canada N6A 5C1. E-mail: qfeng@uwo.ca

© 2009 American Heart Association, Inc.

Circulation is available at <http://circ.ahajournals.org>

DOI: 10.1161/CIRCULATIONAHA.108.846402

Table 1. Morphological Characteristics in WT and nNOS^{-/-} Mice

	WT		nNOS ^{-/-}	
	Sham	MI	Sham	MI
n	28	36	33	49
Body weight, g	27.1±0.8	25.6±0.5	25.0±0.6	25.6±0.4
Age, d	106±8	83±5	111±5	81±4
LVW/BW, mg/g	3.04±0.12	3.66±0.15*	2.46±0.04†	3.39±0.11*
RVW/BW, mg/g	0.86±0.05	0.94±0.05	0.61±0.02†	0.81±0.04*
LVV/BW, μL/g	0.41±0.09	1.80±0.22*	0.36±0.03	1.52±0.23*
Infarct size, %LV	0	35.5±1.3	0	36±1.1

LVW indicates LV weight; BW, body weight; RVW, right ventricular weight; and LVV, LV volume.

Data are mean±SEM.

*P<0.05 vs respective sham; †P<0.05 vs WT sham.

to β-adrenergic stimulation after pharmacological nNOS inhibition. In contrast, 2 recent studies demonstrated that cardiac contractile response to β-adrenergic stimulation was either decreased or unchanged in nNOS^{-/-} mice after MI.^{14,15} Furthermore, mice deficient in nNOS exhibit accelerated left ventricular (LV) remodeling and increased oxidative stress after MI.^{14,15} Thus, it appears that the increases in nNOS expression during heart failure represent a beneficial, cardioprotective response. Indeed, deletion of nNOS has been associated with higher mortality after MI, which is not necessarily caused by heart failure.^{14,15}

There is now emerging evidence that nNOS-derived NO production may play an important role in cardiomyocyte arrhythmogenesis.¹⁶ A recent report by Gonzalez et al¹⁶ found that a deficiency in nNOS was associated with impaired S-nitrosylation of the RyR2, which was associated with a proarrhythmic phenotype in isolated cardiomyocytes. Moreover, it has been suggested that NO may be capable of suppressing spontaneous Ca²⁺ release events in isolated rat cardiomyocytes.¹⁷ However, to the best of our knowledge, no study to date has examined the role of nNOS in arrhythmia *in vivo*.

The present study examined the role of nNOS in cardiac arrhythmia after MI. We hypothesized that nNOS deficiency would increase the incidence of cardiac arrhythmias and decrease survival after MI. Cardiac function, electrophysiology, and survival were studied in wild-type (WT) and nNOS^{-/-} mice after MI. Ca²⁺ transient frequency response and I_{Ca,L} were determined in isolated cardiomyocytes. Furthermore, S-nitrosylation of Ca²⁺ handling proteins was measured in WT and nNOS^{-/-} myocardium after MI. Our data demonstrated for the first time that deficiency in nNOS increases the incidence of ventricular arrhythmias, leading to higher mortality after MI.

Methods

Animals

WT and nNOS^{-/-} mice of C57BL/6 background were purchased from The Jackson Laboratory (Bar Harbor, Me), and a breeding program was implemented at University of Western Ontario animal care facilities. Animals were provided water and food ad libitum and housed in a temperature- and humidity-controlled facility with 12-hour light/dark cycles. The investigations were approved by the institutional Animal Care Committee and conformed to the *Guide for the Care and Use of Mammals in Neuroscience and Behavioral Research* published by the US National Institutes of Health (NIH publication No. 85-23).

the Care and Use of Laboratory Animals published by the US National Institutes of Health (NIH publication No. 85-23).

Telemetry

To detect arrhythmia in mice after MI, ECGs were continuously recorded in freely moving animals with a telemetry system over a 10-day period. As a control, sham-operated mice were subjected to surgical anesthesia and their chests were opened, but they did not receive coronary artery ligation, and ECG was measured over 5 to 10 days.

ECG Monitoring During Myocardial Ischemia and Reperfusion

Short-term monitoring of ECG limb lead I during ischemia/reperfusion (I/R) was performed in anesthetized mice with needle electrodes inserted subcutaneously. ECG was recorded 5 minutes before and throughout the entire I/R protocol with Powerlab Chart 5.0 (AD Instruments, Colorado Springs, Colo).

S-Nitrosylation of Ca²⁺ Handling Proteins

To analyze S-nitrosylation of the L-type Ca²⁺ channels, RyR2, and SERCA2, a 1-mg protein lysate from isolated adult cardiomyocytes was incubated with an antibody targeted to the α1_C subunit of the L-type Ca²⁺ channel (1:100, Santa Cruz Biotechnology, Santa Cruz, Calif), RyR2 (1:100, Affinity Bioreagents, Golden, Colo), or SERCA2 (1:200, Affinity Bioreagents). The immunocomplex was captured using protein A/G-agarose (Santa Cruz), and S-nitrosylation of immunoprecipitated subunits was directly measured by nonreducing Western blot analysis. Samples were then probed with an anti-S-nitrosocysteine antibody (1:2000, Sigma, Oakville, Ontario, Canada) and quantified with densitometry.

Statistical Analysis

All data are expressed as mean±SEM. Statistical significance was assessed by 2-way ANOVA followed by the Bonferroni posthoc test with Prism 4.0 (GraphPad Software, La Jolla, Calif). Incidence of arrhythmia was analyzed with χ² analysis, and survival was analyzed by the Kaplan-Meier method. Differences were considered significant at P<0.05.

Supplemental Methodology

For detailed methods relative to the induction of MI and I/R, hemodynamic measurements, measurement of apoptosis, superoxide anion (O₂⁻) production, telemetry, ECG analysis, adult cardiomyocyte isolation, Ca²⁺ transients, and L-type Ca²⁺ current, see the online-only Data Supplement.

Results

Mortality After MI

WT (n=74) and nNOS^{-/-} (n=114) mice were subjected to MI or sham operation. Animals were excluded from analysis

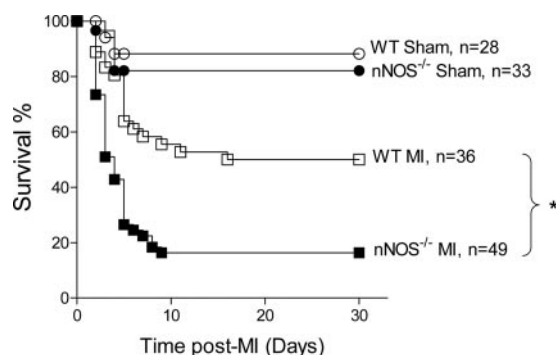


Figure 1. Survival after MI in $nNOS^{-/-}$ and WT mice. Animals were followed up for 30 days after surgery. Post-MI survival was significantly lower in $nNOS^{-/-}$ vs WT mice ($*P<0.01$).

if perioperative death occurred within the first 24 hours after surgery. The remaining 64 WT and 82 $nNOS^{-/-}$ mice were included in the study, and their mortality was followed up for 30 days after surgery. After hemodynamic measurements were obtained, mice were killed. Although sham $nNOS^{-/-}$ mice had a lower ratio of LV weight to body weight than WT sham mice, there were no differences in age, body weight, ratio of LV weight to body weight, and infarct size between $nNOS^{-/-}$ and WT mice subjected to MI (Table 1). MI resulted in a significant increase in mortality in both $nNOS^{-/-}$ and WT mice compared with the sham operation groups ($P<0.01$; Figure 1). Furthermore, the 30-day survival was significantly lower in $nNOS^{-/-}$ mice (8 of 49, 16%) compared with WT mice (18 of 36, 50%; $P<0.01$; Figure 1).

Hemodynamics

To determine whether there were alterations in cardiac function in $nNOS^{-/-}$ mice, heart function was measured in

subgroups at 2 and 30 days after MI with a Millar catheter. In sham mice, there was no significant difference between WT and $nNOS^{-/-}$ mice among any of the measured hemodynamic parameters (Table 2). Two days after MI, there was a significant reduction in systolic LV pressure, in the LV maximal rate of pressure development (dP/dt), and in the maximal rate of relaxation ($-dP/dt$) in WT and $nNOS^{-/-}$ mice. However, LV dP/dt and $-dP/dt$ were both lower in $nNOS^{-/-}$ compared with WT mice. Additionally, 30 days after MI, systolic LV pressure, dP/dt , and $-dP/dt$ also were lower in WT and $nNOS^{-/-}$ mice compared with their respective shams, whereas LV end-diastolic pressure was higher. However, there were no longer differences between surviving WT and $nNOS^{-/-}$ mice among any measured hemodynamic parameters (Table 2).

Superoxide Generation and Apoptosis

Oxidative stress and in particular O_2^- have previously been shown to cause impaired cardiac function in models of heart failure.¹⁸ These effects were associated with increases in apoptotic cell death.¹⁸ We measured myocardial O_2^- production and apoptosis in the peri-infarct region 2 days after MI. O_2^- production, measured by lucigenin assay, was significantly increased in both WT and $nNOS^{-/-}$ mice after MI (Figure 2A). However, the increases in O_2^- production were significantly higher in $nNOS^{-/-}$ compared with WT mice (Figure 2A). Furthermore, MI-induced apoptosis also was significantly higher in $nNOS^{-/-}$ compared with WT mice as measured by terminal deoxynucleotidyl transferase-mediated dUTP nick-end labeling (TUNEL) staining (Figure 2B) and caspase-3 activity (Figure 2C).

Table 2. Hemodynamic Changes in WT and $nNOS^{-/-}$ Mice After MI

	WT		$nNOS^{-/-}$	
	Sham	MI	Sham	MI
2 Days after surgery				
n	7	11	6	11
Heart rate, bpm	467±16	443±16	422±9	432±10
MAP, mm Hg	65.3±3.0	54.5±2.9	73.0±5.7	46.5±3.9*
SLVP, mm Hg	101.1±4.3	78.6±2.3*	104.0±7.0	66.9±3.6*
LVEDP, mm Hg	2.4±0.6	5.3±0.6	3.0±0.8	6.2±1.2
LV dP/dt , mm Hg · s ⁻¹	7181±376	5330±268*	7162±288	4247±365†
LV $-dP/dt$, mm Hg · s ⁻¹	6007±349	4865±283*	6335±341	3765±370*†
30 Days after surgery				
n	7	18	8	12
Heart rate, bpm	399±12	399±12	380±9	413±7
MAP, mm Hg	95.8±5.7	79.3±2.8*	89.2±3.7	71.9±3.1*
SLVP, mm Hg	123.1±8.4	97.9±2.5*	116.3±3.9	94.0±3.2*
LVEDP, mm Hg	6.0±0.7	8.8±1.1*	3.9±0.7	7.1±0.6*
LV dP/dt , mm Hg · s ⁻¹	8785±552	5623±211*	8903±361	5968±333*
LV $-dP/dt$, mm Hg · s ⁻¹	8833±206	5637±191*	8646±195	5854±349*

MAP indicates mean arterial pressure; SLVP, systolic LV pressure; and LVEDP, LV end-diastolic pressure. Data are mean±SEM.

* $P<0.05$ vs respective sham; † $P<0.05$ vs WT MI.

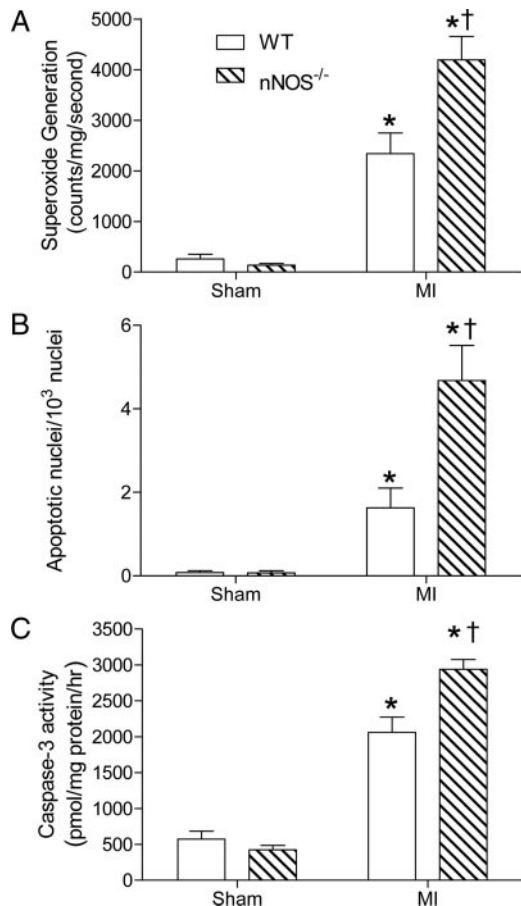


Figure 2. Changes in myocardial apoptosis and superoxide (O_2^-) generation in WT and nNOS^{-/-} mice 2 days after MI. Myocardial O_2^- generation was measured by lucigenin assay (A), and apoptosis was measured by TUNEL staining (B) and caspase-3 activity (C). * $P<0.05$ vs corresponding WT; † $P<0.05$ vs WT plus MI; n=7 to 11 per group.

Ventricular Arrhythmia After MI

To determine whether nNOS deletion was associated with increased ventricular arrhythmia after MI, cardiac ECG was monitored through the use of telemetry in WT and nNOS^{-/-} mice after MI for up to 10 days (Figure 3A). Although there was no change in heart rate among the treatment groups, nNOS^{-/-} mice developed significantly more ventricular arrhythmias than their WT counterparts (Table 3). Additionally, nNOS^{-/-} mice were significantly more likely to develop ventricular fibrillation (VF) in the hour preceding spontaneous death (Figure 3A and Table 3). Sham-operated mice displayed only a few isolated ventricular premature beats, and there were no differences between WT and nNOS^{-/-} mice (Table 3).

nNOS deletion is associated with increased $[Ca^{2+}]_i$,⁷ and elevated $[Ca^{2+}]_i$ has been shown to cause ventricular tachyarrhythmia.¹⁹ The L-type Ca^{2+} channel blocker verapamil was used to examine the role of Ca^{2+} in the increased arrhythmia seen in nNOS^{-/-} mice. Verapamil treatment (0.1 mg/mL in drinking water), which was started 24 hours after MI, significantly reduced ventricular arrhythmias and the incidence of VF in nNOS^{-/-} mice (Table 3).

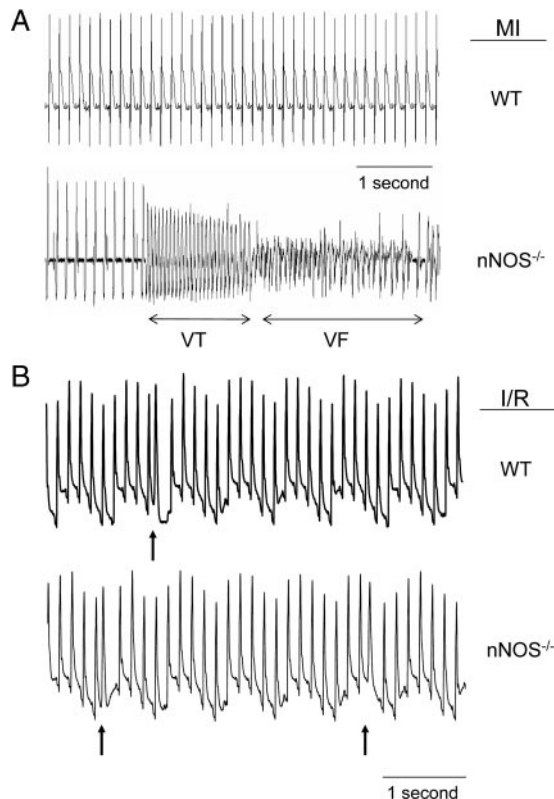


Figure 3. Representative ECG limb lead I tracings of WT and nNOS^{-/-} mice. A, Telemetric recordings of ECG in freely moving mice after MI. Spontaneous monomorphic ventricular tachycardia (VT) degenerating into VF in the nNOS^{-/-} mouse are indicated. B, Ventricular arrhythmic beats (arrows) after myocardial I/R in anesthetized and artificially ventilated mice.

Ventricular Arrhythmia During Myocardial I/R

The role of nNOS in ventricular arrhythmia also was examined in a mouse model of acute myocardial I/R. WT and nNOS^{-/-} mice were subjected to I/R, and cardiac electric activity was monitored with a single-limb lead I ECG. Representative ECG tracings are shown in Figure 3B, and the incidence of arrhythmia is quantified in Table 4. Heart rate was similar across all treatment groups. However, the numbers of singlet and doublet ventricular premature beats and of ventricular tachycardias were significantly higher in nNOS^{-/-} mice compared with their WT counterparts. Treatment with verapamil (0.02 mg/kg IP) after the start of ischemia significantly reduced the incidence of ventricular tachycardia and the number of ventricular premature beats in WT and nNOS^{-/-} mice (Table 4). Thus, alterations in Ca^{2+} handling may contribute to the increased susceptibility to ventricular arrhythmia seen in these animals during I/R.

Intracellular Ca^{2+} Transients

To investigate Ca^{2+} handling mechanisms, we measured Ca^{2+} transients in fura-2-loaded ventricular myocytes isolated from WT and nNOS^{-/-} mice. Peak $[Ca^{2+}]_i$ was significantly higher in nNOS^{-/-} compared with WT cardiomyocytes (Figure 4). Furthermore, pharmacological inhibition of nNOS with N⁵-(1-imino-3-butenyl)-L-ornithine (L-VNIO; 100 μ mol/L) increased peak $[Ca^{2+}]_i$ in WT but not nNOS^{-/-} cardiomyocytes (Figure 4A through 4C). Conversely, treatment with the NO

Table 3. Electrophysiological Parameters From Telemetric Recordings in WT and nNOS^{-/-} Mice After MI in the Presence and Absence of Verapamil (0.1 mg/mL in Drinking Water)

	Sham		Vehicle		Verapamil	
	WT	nNOS ^{-/-}	WT	nNOS ^{-/-}	WT	nNOS ^{-/-}
n	3	3	6	6	6	6
Heart rate, bpm						
Before MI	600±35	640±20	571±42	547±16	550±42	536±38
After MI	NA	NA	564±30	541±56	553±3	541±48
Ventricular arrhythmias, n/h	0.14±0.07	0.18±0.04	0.7±0.3	4.6±1.9*	0.3±0.1	0.7±0.3†
Incidence of VF, % (n/N)	0	0	0 (0/6)	67 (4/6)*	0 (0/6)	17 (1/6)†
Total duration of VF, s	0	0	0	15.0±5.8*	0	0.9±0.9†

Mice were randomly assigned to vehicle and verapamil treatment groups. Data are mean±SEM.

*P<0.05 vs WT vehicle; †P<0.05 vs nNOS^{-/-} vehicle.

donor S-nitroso N-acetyl-penicillamine (SNAP; 10 μmol/L), significantly reduced peak [Ca²⁺]_i in both WT and nNOS^{-/-} cardiomyocytes (Figure 4D through 4F).

To determine whether the difference in Ca²⁺ transients is frequency dependent, WT and nNOS^{-/-} cardiomyocytes were paced over a range of frequencies (0.5 to 4 Hz; Figure 5A through 5D). nNOS^{-/-} cardiomyocytes exhibited consistently higher diastolic Ca²⁺ than WT cardiomyocytes (Figure 5A). Additionally, nNOS^{-/-} cardiomyocytes exhibited significantly higher systolic Ca²⁺ levels at 0.5, 1, and 2 Hz (Figure 5B).

Patch-Clamp Recordings of L-Type Ca²⁺ Channel Currents

To determine whether the changes in the evoked Ca²⁺ transients were caused by regulation of Ca²⁺ current, we next

used perforated patch-clamp recordings to characterize L-type Ca²⁺ current in isolated myocytes. Depolarization of cells elicited the characteristic L-type Ca²⁺ current, evident as a transient inward current, which was reversibly blocked by verapamil (1 μmol/L; 5 cells; not shown). The average access resistance in perforated patch configuration was 18±1 mol/LΩ (from 58 cells in 25 different cell preparations). Treatment of WT cardiomyocytes with the selective nNOS inhibitor L-VNIO (100 μmol/L) for 30 seconds caused a marked and consistent increase in the amplitude of the Ca²⁺ current (Figure 6A, left). The peak effect was evident within 20 seconds of the application of L-VNIO, and recovery occurred over several minutes. When cardiomyocytes isolated from nNOS^{-/-} mice were studied, Ca²⁺ currents were

Table 4. Electrophysiological Parameters in WT and nNOS^{-/-} Mice During I/R in the Presence and Absence of Verapamil (0.02 mg/kg IP)

	Vehicle		Verapamil	
	WT	nNOS ^{-/-}	WT	nNOS ^{-/-}
n	7	7	6	6
Heart rate, bpm				
Basal	326±11	314±16	304±23	307±25
Ischemia	338±27	354±16	348±27	359±19
Reperfusion	291±20	326±13	308±29	309±22
VPBs (singles and doublets)				
Basal	0±0	0±0	0±0	0±0
Ischemia	0.9±0.6	8.3±1.4	2.3±1.6	1.8±0.3
Reperfusion	9.0±3.3	21.7±4.3*	1.8±1.0	5.2±3.1†
VT, counts				
Basal	0±0	0±0	0±0	0±0
Ischemia	0.3±0.2	4.4±1.8*	0.3±0.2	0.3±0.2†
Reperfusion	5.6±2.2	18.0±5.6*	0.5±0.2	2.5±1.1†
Total VT duration, s				
Basal	0±0	0±0	0±0	0±0
Ischemia	0.8±0.6	22.7±12.6	1.7±1.1	2.0±1.3
Reperfusion	15.3±7.6	74.4±23.2*	1.2±0.8	4.9±1.9†

VPBs indicates ventricular premature beats; VT, ventricular tachycardia. Mice were anesthetized and artificially ventilated. Mice were randomly assigned to vehicle and verapamil treatment groups. Data are mean±SEM.

*P<0.05 vs WT vehicle; †P<0.05 vs nNOS^{-/-} vehicle.

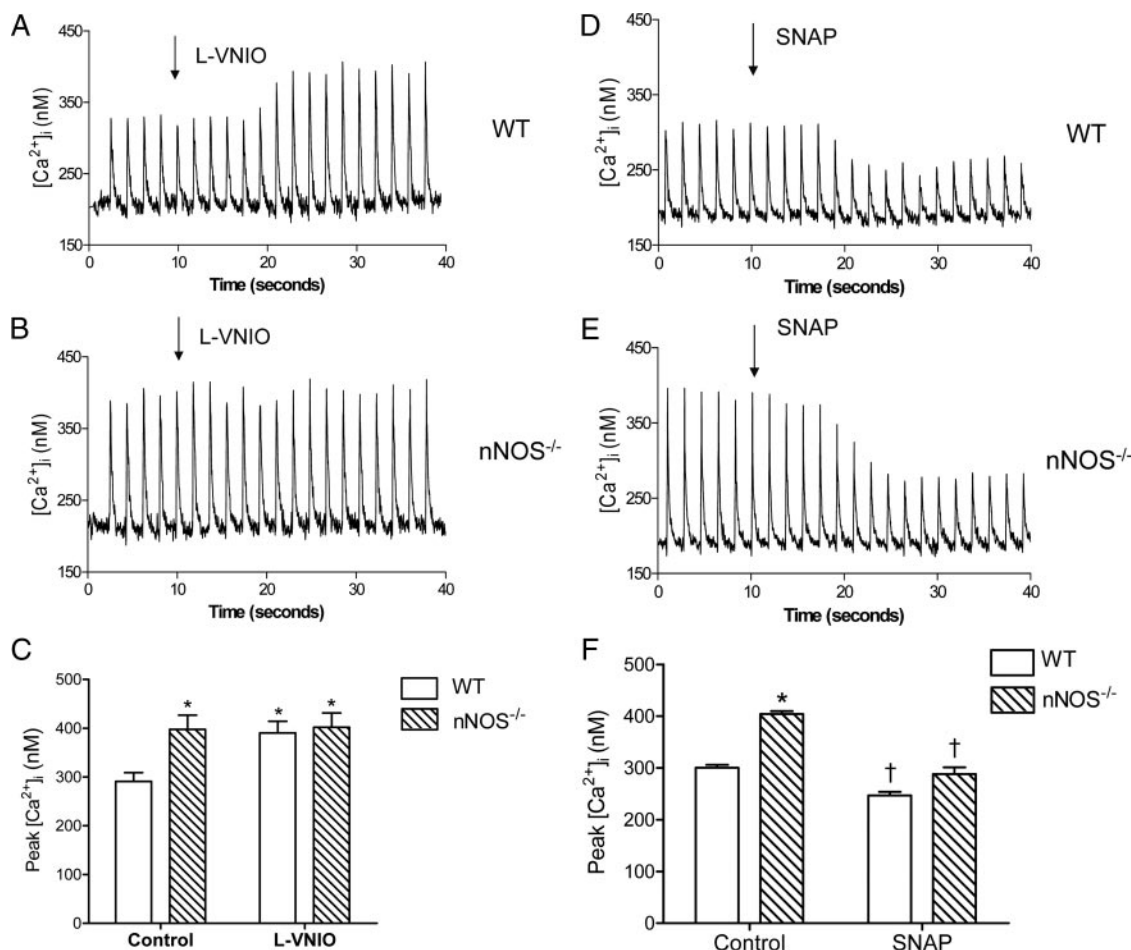


Figure 4. Intracellular Ca²⁺ transients in WT and nNOS^{-/-} cardiomyocytes with and without the nNOS inhibitor L-VNIO (A, B) or the NO donor SNAP (D, E). C, Average peak intracellular Ca²⁺ concentration ([Ca²⁺]_i) before and after treatment with L-VNIO. *P<0.05 vs WT control; n=15 to 18 from 9 mice per group. F, Average peak intracellular Ca²⁺ concentration ([Ca²⁺]_i) before and after treatment with SNAP. *P<0.05 vs WT control; †P<0.05 vs genotype control; n=7 to 9 from 6 mice per group.

significantly larger than those from WT mice (Figure 6A, right, and Figure 6B). Furthermore, treatment of the nNOS^{-/-} cells with L-VNIO for comparable times did not result in a significant change in amplitude of the Ca²⁺ current, in contrast to that seen for WT cells (Figure 6A and 6B). To confirm the action of NO, we applied SNAP (10 μmol/L) during the recording of L-type Ca²⁺ current. In WT and nNOS^{-/-} cardiomyocytes, Ca²⁺ currents were significantly inhibited by SNAP, which was reversible (Figure 7A and 7B).

S-Nitrosylation of Ca²⁺ Handling Proteins

After MI

To determine whether nNOS-derived NO directly interacted with proteins involved in [Ca²⁺]_i regulation, we measured S-nitrosylation of the α_{1c} subunit of the L-type Ca²⁺ channel, RyR2, and SERCA2 in the LV myocardium 5 days after MI using immunoprecipitation followed by Western blotting. S-nitrosylation of all 3 proteins was detectable in WT and nNOS^{-/-} myocardium (Figure 8). However, S-nitrosylation was significantly reduced in nNOS^{-/-} compared with WT hearts (Figure 8), suggesting decreased S-nitrosylation of the L-type Ca²⁺ channel, RyR2, and SERCA2 in nNOS^{-/-} mice after MI.

Discussion

In the present study, we showed that nNOS deletion was associated with increased mortality, O₂⁻ production, and apoptosis in surviving mice and decreased contractility after MI. A novel finding from our study is that ventricular arrhythmias were higher in nNOS^{-/-} than WT mice after MI. Deficiency in nNOS increased Ca²⁺ transient amplitude and L-type Ca²⁺ channel activity and increased diastolic Ca²⁺ levels in cardiomyocytes. S-nitrosylation of the L-type Ca²⁺ channel, RyR2, and SERCA2 in the myocardium was decreased after MI. These data suggest that nNOS has a beneficial role in the regulation of [Ca²⁺]_i via S-nitrosylation of Ca²⁺ handling proteins, leading to reductions in ventricular arrhythmias and death after MI.

Two previous investigations have examined the role of nNOS after MI.^{14,15} In these studies, ventricular remodeling as measured by LV volume and myocyte size was increased in nNOS^{-/-} mice. Although the inotropic response to dobutamine was attenuated, cardiac function, including LV dP/dt, LV end-diastolic pressure, and LV ejection fraction, was not significantly different between nNOS^{-/-} and WT mice 4 weeks after MI.^{14,15} Consistent with these reports, we did not find a significant impairment in cardiac function between

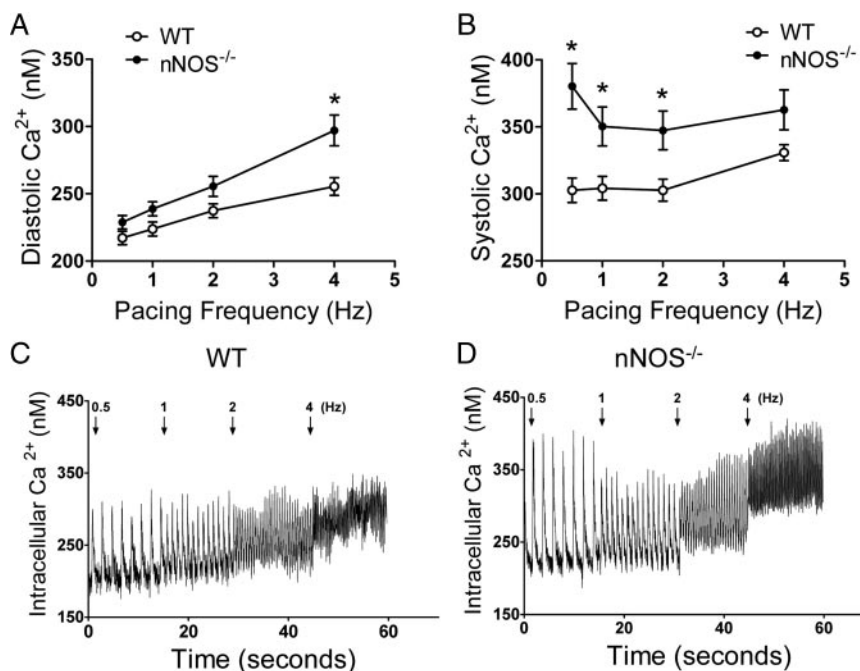


Figure 5. Diastolic (A) and systolic (B) Ca^{2+} responses to increasing frequency of stimulation in WT and $\text{nNOS}^{-/-}$ cardiomyocytes. Representative tracings from WT (C) and $\text{nNOS}^{-/-}$ (D) cardiomyocytes. * $P<0.05$ vs respective WT counterpart; $n=10$ to 17 cells from 4 mice per group.

surviving $\text{nNOS}^{-/-}$ and WT mice 4 weeks after MI. However, survival was significantly decreased in $\text{nNOS}^{-/-}$ mice after MI. Because most animals died within a few days after MI, we also measured cardiac function 2 days after MI and showed that cardiac function was lower in $\text{nNOS}^{-/-}$ compared with WT mice. Lower cardiac function was associated with higher NAD(P)H oxidase-dependent O_2^- generation and myocardial apoptosis. Importantly, during measurements of cardiac function, more ventricular premature beats were

observed in $\text{nNOS}^{-/-}$ mice, which led to our investigation of cardiac arrhythmia.

Perhaps the most striking observation from this study is that nNOS deletion was associated with more ventricular arrhythmias after MI. Mounting evidence suggests that nNOS is beneficial after MI.^{14,15} However, mechanisms responsible for the beneficial effects of nNOS are not fully understood. Recently, Gonzalez et al¹⁶ reported sarcoplasmic reticulum Ca^{2+} leak and an arrhythmogenic phenotype in isolated $\text{nNOS}^{-/-}$ cardiomyocytes. Our laboratory, to the best of our knowledge, provides the first *in vivo* evidence of increased

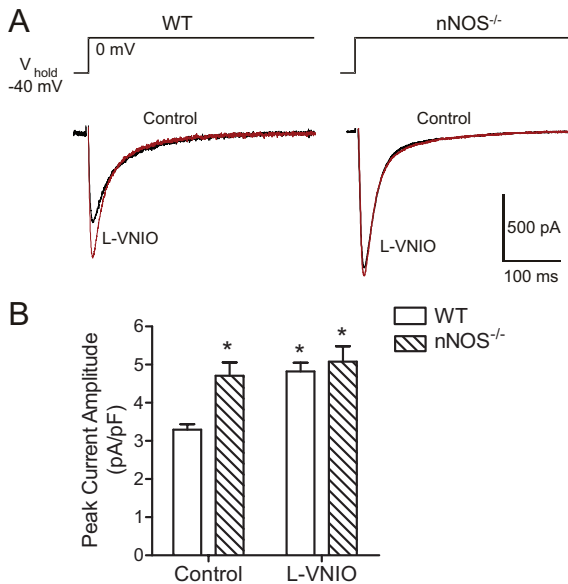


Figure 6. L-type Ca^{2+} current in WT and $\text{nNOS}^{-/-}$ cardiomyocytes in the presence and absence of the nNOS inhibitor L-VNIO. A, Depolarization elicited transient inward Ca^{2+} current that was enhanced and prolonged in $\text{nNOS}^{-/-}$ cardiomyocytes and in WT myocytes treated with L-VNIO ($100 \mu\text{mol/L}$). B, Quantitative summary of peak amplitude of L-type Ca^{2+} current. Red traces are for Ca^{2+} current in the presence of L-VNIO. * $P<0.05$ vs WT control; $n=15$ cells from 5 mice per group.

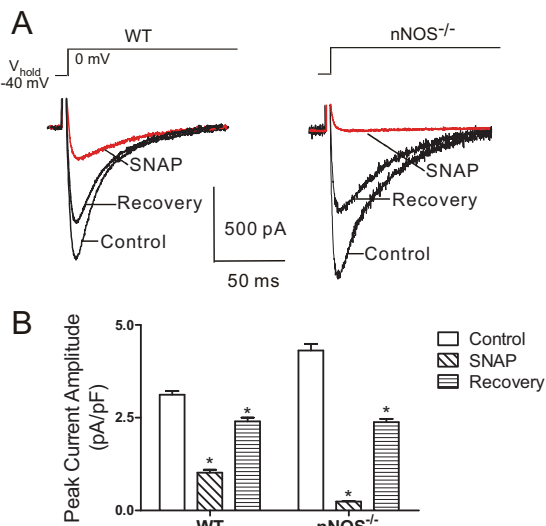


Figure 7. L-type Ca^{2+} current in WT and $\text{nNOS}^{-/-}$ cardiomyocytes in the presence and absence of the NO donor SNAP ($10 \mu\text{mol/L}$). A, Depolarization elicited transient inward Ca^{2+} current that was diminished in WT and $\text{nNOS}^{-/-}$ myocytes by the addition of SNAP. Overlapping traces are shown. Red traces are for Ca^{2+} current in the presence of SNAP. B, Quantitative summary of peak amplitude of L-type Ca^{2+} current. * $P<0.05$ vs respective untreated controls; $n=10$ to 12 from 5 mice per group.

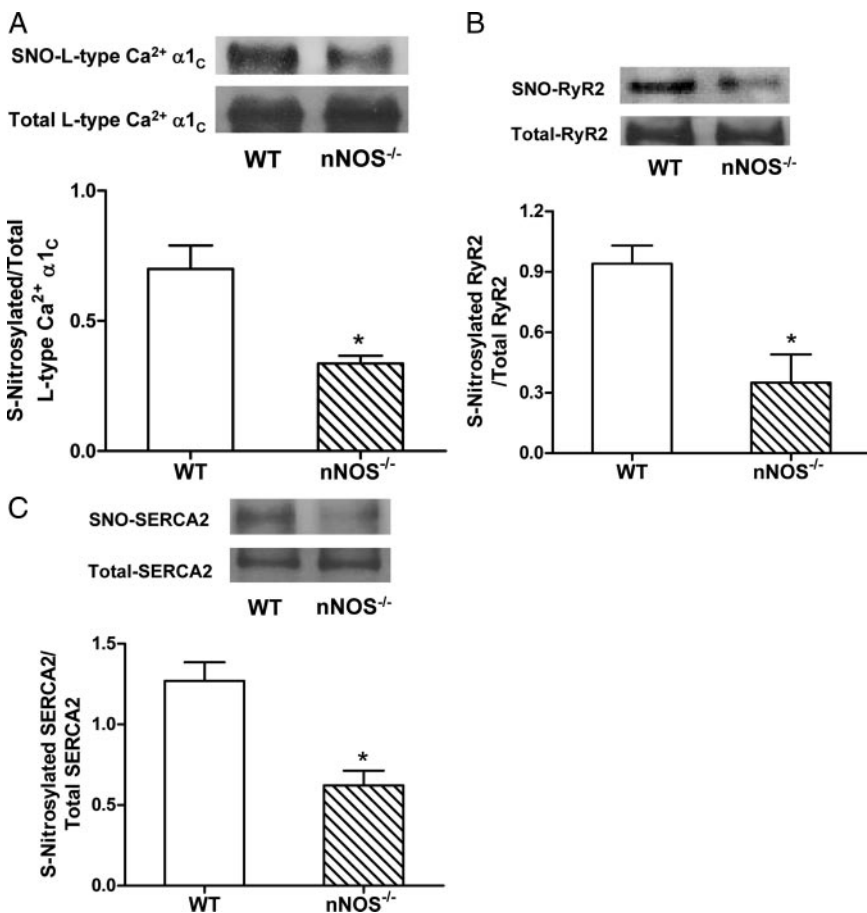


Figure 8. S-nitrosylation of the Ca^{2+} handling proteins in WT and $\text{nNOS}^{-/-}$ myocardium after MI. Samples were immunoprecipitated with antibodies targeted to the $\alpha 1_c$ subunit of the L-type Ca^{2+} channel, RyR2, or SERCA2 and subjected to Western blot analysis with an anti-nitroso cysteine antibody.

* $P < 0.05$ vs WT; $n=3$ to 6 mice per group.

ventricular arrhythmia in $\text{nNOS}^{-/-}$ mice. Deletion of nNOS resulted in higher incidences of ventricular tachycardia and/or VF after myocardial I/R and MI. Interestingly, $\text{nNOS}^{-/-}$ mice are known to have vastly accelerated mortality with aging (>10 months old) even in the absence of MI.²⁰ The present study was done in mice 3 to 4 months of age, and no difference in arrhythmia was detected between sham-operated WT and $\text{nNOS}^{-/-}$ mice. It is possible that, with aging, $\text{nNOS}^{-/-}$ mice are more susceptible to arrhythmia, which may be responsible for increased mortality. Indeed, aging has been associated with an increased susceptibility to Ca^{2+} overload in rabbits and rats.^{21–23}

nNOS deletion is associated with higher L-type Ca^{2+} channel activity, diastolic Ca^{2+} elevations, and higher $[\text{Ca}^{2+}]_i$ in myocytes, which are known to cause ventricular arrhythmia.¹⁹ Therefore, we examined the effects of the L-type Ca^{2+} channel blocker verapamil on ventricular arrhythmias in $\text{nNOS}^{-/-}$ and WT mice during I/R and after MI. Although primarily used clinically for supraventricular arrhythmias, verapamil is also known to prevent VF caused by ischemia in patients with coronary artery disease and may reduce ventricular tachyarrhythmias associated with I/R.^{24,25} As expected, verapamil treatment significantly reduced I/R-induced ventricular tachyarrhythmia and reduced the incidence of VF after MI. These data suggest a role for altered Ca^{2+} handling in the increased cardiac arrhythmia in $\text{nNOS}^{-/-}$ mice after MI.

To further understand the role of nNOS in the regulation of $[\text{Ca}^{2+}]_i$, Ca^{2+} transients and L-type Ca^{2+} channel activity were

determined. We found that pharmacological inhibition and genetic deletion of nNOS increased $[\text{Ca}^{2+}]_i$ in isolated mouse cardiomyocytes. These observations are in agreement with the work of Sears et al,⁷ who also showed higher Ca^{2+} transient amplitude and L-type Ca^{2+} current in $\text{nNOS}^{-/-}$ cardiomyocytes. Although others have failed to observe alterations in Ca^{2+} transients in $\text{nNOS}^{-/-}$ mice,^{26,27} a recent report by Burkard and colleagues⁶ provided strong evidence of a role for nNOS in the regulation of $[\text{Ca}^{2+}]_i$ in cardiomyocytes. In that study, the authors observed reductions in Ca^{2+} transient and L-type Ca^{2+} current amplitude in cardiomyocytes overexpressing nNOS. Similarly, we observed reductions in Ca^{2+} transient amplitude, as well as L-type Ca^{2+} current amplitude, after administration of the NO donor SNAP in both WT and $\text{nNOS}^{-/-}$ cardiomyocytes. These observations, coupled with the initial work of Sears et al,⁷ provide compelling evidence of a role for nNOS-derived NO production in the inhibition of the L-type Ca^{2+} channel and regulation of $[\text{Ca}^{2+}]_i$ in cardiomyocytes. Interestingly, elevated $[\text{Ca}^{2+}]_i$ such as that seen in $\text{nNOS}^{-/-}$ cardiomyocytes is thought to lead to Ca^{2+} overload, thereby triggering the initiation of ventricular arrhythmia.¹⁹ Thus, it is possible that the mechanism by which nNOS reduces ventricular arrhythmia is through this NO-dependent inhibition of the L-type Ca^{2+} channel and subsequent reduction in Ca^{2+} overload.

nNOS-derived NO also may play an important role in preventing diastolic Ca^{2+} leak in cardiomyocytes, particularly at higher pacing frequencies.¹⁶ In agreement with this, we

found that diastolic Ca^{2+} was increased in nNOS^{-/-} compared with WT cardiomyocytes when paced at higher frequencies. Diastolic Ca^{2+} leak is associated with spontaneous Ca^{2+} waves, which are capable of generating delayed afterdepolarizations.^{16,28} In fact, at higher pacing rates, this diastolic Ca^{2+} elevation appears to diminish contractile reserve and the peak $[\text{Ca}^{2+}]_i$ levels because nNOS^{-/-} cardiomyocytes are no longer significantly different from their WT counterparts.¹⁶ Thus, the arrhythmia seen in nNOS^{-/-} mice may result from diastolic Ca^{2+} leak, in addition to Ca^{2+} overload.

S-nitrosylation of the L-type Ca^{2+} channel has recently been observed in the membrane fractions of mouse hearts, and S-nitrosylation of the L-type Ca^{2+} channel results in a decrease in activity of the channel.²⁹ Moreover, deficiency in S-nitrosylation of RyR2 is associated with sarcoplasmic reticulum Ca^{2+} leak and arrhythmogenesis,¹⁶ whereas S-nitrosylation of SERCA2 appears to increase activity of the enzyme.²⁹ In the present study, we demonstrated an important role for nNOS in the S-nitrosylation of $[\text{Ca}^{2+}]_i$ handling proteins, including the L-type Ca^{2+} channel subunit $\alpha 1_C$, RyR2, and SERCA2, in the LV myocardium after MI. S-nitrosylation of these proteins would prevent Ca^{2+} overload and subsequent ventricular arrhythmias. Indeed, nNOS is particularly suited to regulate Ca^{2+} because increases in $[\text{Ca}^{2+}]_i$ also increase nNOS-derived NO production. This negative feedback via S-nitrosylation would, in turn, protect the cardiomyocyte from arrhythmogenesis. However, one cannot rule out potential effects of NO not attributable to S-nitrosylation. L-type Ca^{2+} channels, RyR2, and SERCA2 are subject to extensive redox regulation by reactive oxygen species.^{30,31} In the present study, we demonstrated that myocardial reactive oxygen species levels were increased in nNOS^{-/-} mice, suggesting an antioxidant effect of nNOS.³² It is possible that increased reactive oxygen species production may contribute to the changes in Ca^{2+} seen in nNOS^{-/-} cardiomyocytes. Moreover, NO also has been reported to modulate the L-type Ca^{2+} channel via cGMP.^{31,33} Thus, although S-nitrosylation is an important contributor to the altered Ca^{2+} handling and ventricular arrhythmia in nNOS^{-/-} mice, the precise regulation of Ca^{2+} handling proteins is complex and may involve reactive oxygen species and other factors.

Finally, although this study has examined the role of nNOS-derived NO in the control of $[\text{Ca}^{2+}]_i$ and ventricular arrhythmia, the contribution from eNOS cannot be excluded. This is particularly relevant given the residual S-nitrosylation of the L-type Ca^{2+} channel, RyR2, and SERCA2 seen even in the absence of nNOS. eNOS-derived NO has been reported to contribute to S-nitrosylation of the L-type Ca^{2+} channel in mouse hearts.³⁴ However, Gonzalez et al¹⁶ did not find any changes in S-nitrosylation of the RyR2 in eNOS^{-/-} cardiomyocytes, suggesting that eNOS is not involved in the S-nitrosylation of RyR2 under normal physiological conditions. In the failing myocardium, eNOS expression is upregulated.³⁵ Whether increased eNOS expression after MI leads to S-nitrosylation of the RyR2 and inhibits ventricular arrhythmia requires further investigation.

Conclusions

Our results demonstrate that nNOS-derived NO is beneficial in mouse models of I/R and MI. Deficiency in nNOS decreases cardiac function and increases ventricular arrhythmias, leading to a higher mortality after MI. The finding that nNOS deletion increases ventricular arrhythmia suggests an antiarrhythmic mechanism of nNOS after MI.

Sources of Funding

This study was supported by grants from the Heart and Stroke Foundation of Ontario (T-6040 to Dr Feng) and the Canadian Institutes of Health Research (MOP-64395 to Dr Feng, MOP-10019 to Dr Sims). Dr Burger was supported by an Ontario Graduate Scholarship Award. Dr Feng is a Heart and Stroke Foundation of Ontario career investigator.

Disclosures

None.

References

1. Schmidt HH, Murad F. Purification and characterization of a human NO synthase. *Biochem Biophys Res Commun*. 1991;181:1372-1377.
2. Schmidt HH, Gagne GD, Nakane M, Pollock JS, Miller MF, Murad F. Mapping of neural nitric oxide synthase in the rat suggests frequent co-localization with NADPH diaphorase but not with soluble guanylyl cyclase, and novel paraneuronal functions for nitrinergic signal transduction. *J Histochem Cytochem*. 1992;40:1439-1456.
3. Wang Y, Marsden PA. Nitric oxide synthases: gene structure and regulation. *Adv Pharmacol*. 1995;34:71-90.
4. Xu KY, Huso DL, Dawson TM, Bredt DS, Becker LC. Nitric oxide synthase in cardiac sarcoplasmic reticulum. *Proc Natl Acad Sci U S A*. 1999;96:657-662.
5. Damy T, Ratajczak P, Shah AM, Camors E, Marty I, Hasenfuss G, Marotte F, Samuel JL, Heymes C. Increased neuronal nitric oxide synthase-derived NO production in the failing human heart. *Lancet*. 2004;363:1365-1367.
6. Burkard N, Rokita AG, Kaufmann SG, Hallhuber M, Wu R, Hu K, Hofmann U, Bonz A, Frantz S, Cartwright EJ, Neyses L, Maier LS, Maier SK, Renne T, Schuh K, Ritter O. Conditional neuronal nitric oxide synthase overexpression impairs myocardial contractility. *Circ Res*. 2007;100:e32-e44.
7. Sears CE, Bryant SM, Ashley EA, Lygate CA, Rakovic S, Wallis HL, Neubauer S, Terrar DA, Casadei B. Cardiac neuronal nitric oxide synthase isoform regulates myocardial contraction and calcium handling. *Circ Res*. 2003;92:e52-e59.
8. Ashley EA, Sears CE, Bryant SM, Watkins HC, Casadei B. Cardiac nitric oxide synthase 1 regulates basal and beta-adrenergic contractility in murine ventricular myocytes. *Circulation*. 2002;105:3011-3016.
9. Zhang YH, Zhang MH, Sears CE, Emanuel K, Redwood C, El-Armouche A, Kranias EG, Casadei B. Reduced phospholamban phosphorylation is associated with impaired relaxation in left ventricular myocytes from neuronal NO synthase-deficient mice. *Circ Res*. 2008;102:242-249.
10. Heaton DA, Lei M, Li D, Golding S, Dawson TA, Mohan RM, Paterson DJ. Remodeling of the cardiac pacemaker L-type calcium current and its beta-adrenergic responsiveness in hypertension after neuronal NO synthase gene transfer. *Hypertension*. 2006;48:443-452.
11. Casadei B. The emerging role of neuronal nitric oxide synthase in the regulation of myocardial function. *Exp Physiol*. 2006;91:943-955.
12. Damy T, Ratajczak P, Robidel E, Bendall JK, Oliviero P, Boczkowski J, Ebrahimian T, Marotte F, Samuel JL, Heymes C. Up-regulation of cardiac nitric oxide synthase 1-derived nitric oxide after myocardial infarction in senescent rats. *FASEB J*. 2003;17:1934-1936.
13. Bendall JK, Damy T, Ratajczak P, Loyer X, Monceau V, Marty I, Milliez P, Robidel E, Marotte F, Samuel JL, Heymes C. Role of myocardial neuronal nitric oxide synthase-derived nitric oxide in beta-adrenergic hyporesponsiveness after myocardial infarction-induced heart failure in rat. *Circulation*. 2004;110:2368-2375.
14. Dawson D, Lygate CA, Zhang MH, Hulbert K, Neubauer S, Casadei B. nNOS gene deletion exacerbates pathological left ventricular remodeling and functional deterioration after myocardial infarction. *Circulation*. 2005;112:3729-3737.

15. Saraiva RM, Minhas KM, Raju SV, Barouch LA, Pitz E, Schuleri KH, Vandegaer K, Li D, Hare JM. Deficiency of neuronal nitric oxide synthase increases mortality and cardiac remodeling after myocardial infarction: role of nitroso-redox equilibrium. *Circulation*. 2005;112:3415–3422.
16. Gonzalez DR, Beigi F, Treuer AV, Hare JM. Deficient ryanodine receptor S-nitrosylation increases sarcoplasmic reticulum calcium leak and arrhythmogenesis in cardiomyocytes. *Proc Natl Acad Sci U S A*. 2007;104:20612–20617.
17. Meszaros LG. Suppression of spontaneous calcium release events by nitric oxide in rat ventricular myocytes. *J Muscle Res Cell Motil*. 2004;25:604–605.
18. Qin F, Simeone M, Patel R. Inhibition of NADPH oxidase reduces myocardial oxidative stress and apoptosis and improves cardiac function in heart failure after myocardial infarction. *Free Radic Biol Med*. 2007;43:271–281.
19. Zaugg CE. Current concepts on ventricular fibrillation: a vicious circle of cardiomyocyte calcium overload in the initiation, maintenance, and termination of ventricular fibrillation. *Indian Pacing Electrophysiol J*. 2004;4:85–92.
20. Barouch LA, Cappola TP, Harrison RW, Crone JK, Rodriguez ER, Burnett AL, Hare JM. Combined loss of neuronal and endothelial nitric oxide synthase causes premature mortality and age-related hypertrophic cardiac remodeling in mice. *J Mol Cell Cardiol*. 2003;35:637–644.
21. Ataka K, Chen D, Levitsky S, Jimenez E, Feinberg H. Effect of aging on intracellular Ca^{2+} , pH, and contractility during ischemia and reperfusion. *Circulation*. 1992;86(suppl):II-371–II-376.
22. Carbonin PU, Di Gennaro M, Pahor M, Bernabei R, Sgadari A, Gambassi G Jr. Cardiac aging, calcium overload, and arrhythmias. *Exp Gerontol*. 1990;25:261–268.
23. Frolkis VV, Frolkis RA, Mkhitarian LS, Shevchuk VG, Fraifeld VE, Vakulenko LG, Syrov I. Contractile function and Ca^{2+} transport system of myocardium in ageing. *Gerontology*. 1988;34:64–74.
24. Clusin WT. Calcium and cardiac arrhythmias: DADs, EADs, and alternans. *Crit Rev Clin Lab Sci*. 2003;40:337–375.
25. Lu HR, Yang P, Remeyen P, Saele A, Dai DZ, De Clerck F. Ischemia/reperfusion-induced arrhythmias in anaesthetized rats: a role of Na^+ and Ca^{2+} influx. *Eur J Pharmacol*. 1999;365:233–239.
26. Khan SA, Skaf MW, Harrison RW, Lee K, Minhas KM, Kumar A, Bradley M, Shoukas AA, Berkowitz DE, Hare JM. Nitric oxide regulation of myocardial contractility and calcium cycling: independent impact of neuronal and endothelial nitric oxide synthases. *Circ Res*. 2003;92:1322–1329.
27. Barouch LA, Harrison RW, Skaf MW, Rosas GO, Cappola TP, Kobeissi ZA, Hobai IA, Lemmon CA, Burnett AL, O'Rourke B, Rodriguez ER, Huang PL, Lima JA, Berkowitz DE, Hare JM. Nitric oxide regulates the heart by spatial confinement of nitric oxide synthase isoforms. *Nature*. 2002;416:337–339.
28. Schlotthauer K, Bers DM. Sarcoplasmic reticulum Ca^{2+} release causes myocyte depolarization: underlying mechanism and threshold for triggered action potentials. *Circ Res*. 2000;87:774–780.
29. Sun J, Morgan M, Shen RF, Steenbergen C, Murphy E. Preconditioning results in S-nitrosylation of proteins involved in regulation of mitochondrial energetics and calcium transport. *Circ Res*. 2007;101:1155–1163.
30. Hool LC, Corry B. Redox control of calcium channels: from mechanisms to therapeutic opportunities. *Antioxid Redox Signal*. 2007;9:409–435.
31. Campbell DL, Stamler JS, Strauss HC. Redox modulation of L-type calcium channels in ferret ventricular myocytes: dual mechanism regulation by nitric oxide and S-nitrosothiols. *J Gen Physiol*. 1996;108:277–293.
32. Khan SA, Lee K, Minhas KM, Gonzalez DR, Raju SV, Tejani AD, Li D, Berkowitz DE, Hare JM. Neuronal nitric oxide synthase negatively regulates xanthine oxidoreductase inhibition of cardiac excitation-contraction coupling. *Proc Natl Acad Sci U S A*. 2004;101:15944–15948.
33. Gallo MP, Malan D, Bedendi I, Biasin C, Alloatti G, Levi RC. Regulation of cardiac calcium current by NO and cGMP-modulating agents. *Pflugers Arch*. 2001;441:621–628.
34. Sun J, Picht E, Ginsburg KS, Bers DM, Steenbergen C, Murphy E. Hypercontractile female hearts exhibit increased S-nitrosylation of the L-type Ca^{2+} channel alpha1 subunit and reduced ischemia/reperfusion injury. *Circ Res*. 2006;98:403–411.
35. Stein B, Eschenhagen T, Rudiger J, Scholz H, Forstermann U, Gath I. Increased expression of constitutive nitric oxide synthase III, but not inducible nitric oxide synthase II, in human heart failure. *J Am Coll Cardiol*. 1998;32:1179–1186.

CLINICAL PERSPECTIVE

Ventricular arrhythmia is a common cause of death after myocardial infarction (MI). Cardiomyocyte Ca^{2+} overload and diastolic Ca^{2+} leak are important mechanisms responsible for afterdepolarization and triggered activity leading to ventricular arrhythmia after MI. Emerging evidence suggests that neuronal nitric oxide synthase (nNOS) may inhibit arrhythmogenesis by maintaining intracellular Ca^{2+} homeostasis in cardiomyocytes. However, the role of nNOS in ventricular arrhythmia after MI in vivo is not clear. In the present study, we demonstrated that nNOS deletion was associated with increased mortality, reactive oxygen species production, and apoptosis after MI. A novel finding from our study is that ventricular arrhythmias were significantly higher in nNOS^{-/-} compared with wild-type mice after MI. Deficiency in nNOS increased Ca^{2+} transient amplitude and L-type Ca^{2+} channel activity and increased diastolic Ca^{2+} levels in cardiomyocytes. Lack of nNOS decreased S-nitrosylation of the L-type Ca^{2+} channel, ryanodine receptor Ca^{2+} release channel, and SERCA2 in the myocardium after MI. Thus, nNOS has a beneficial role in Ca^{2+} homeostasis via S-nitrosylation of Ca^{2+} handling proteins, leading to reductions in ventricular arrhythmias and death after MI. Our study provides new insights into the protective role of nNOS in arrhythmogenesis and may have therapeutic implications after MI.

Neuronal Nitric Oxide Synthase Protects Against Myocardial Infarction-Induced Ventricular Arrhythmia and Mortality in Mice

Burger DE, et al.

SUPPLEMENTAL MATERIAL

Methods

Induction of MI and Ischemia/Reperfusion (I/R)

Adult nNOS^{-/-} mice and their WT littermates (males, 3-4 months old) were randomly selected to undergo coronary artery ligation to induce MI or sham surgery (same procedure without coronary artery ligation) as described previously¹. Mice were anesthetized, intubated, and mechanically ventilated. A left intercostal thoracotomy was performed and the left coronary artery was ligated by placing a suture (8-0) around it. The lungs were then hyper-inflated using positive end-expiratory pressures (3 cm H₂O), and the thorax was closed. Infarct size was determined at the end of the study¹. In the case of myocardial I/R, the left coronary artery was occluded for 45 minutes to induce ischemia and the suture was loosened to allow for reperfusion for 45 minutes.

Hemodynamic Measurements

Heart function was measured 2 and 30 days post-MI in anesthetized mice as described previously². Briefly, a Millar pressure transducer catheter (1.4-Fr) was placed in the right carotid artery for measurement of arterial blood pressure and heart rate. The catheter was then advanced into the left ventricle for measurement of left ventricular (LV) systolic and end-diastolic

pressures, as well as the LV maximal rate of pressure development ($+dP/dt$) and maximal rate of pressure relaxation ($-dP/dt$). All measurements were recorded using PowerLab Chart Program (ADIInstruments, Colorado Springs, CO).

Measurement of Apoptosis and Superoxide Production

Caspase-3 activity was measured using a caspase-3 assay kit (BIOMOL, Plymouth Meeting, PA) as previously described³. Terminal deoxynucleotidyl transferase d-UTP nick end labeling (TUNEL) staining was performed on paraffin-embedded heart sections using an In Situ Cell Death Detection Kit (Roche, Indianapolis, IN) as previously reported³. NADH-dependent O_2^- generation was measured in cell lysates by lucigenin-enhanced chemiluminescence (20 µg of protein, 100 µmol/L β-NADH, 5 µmol/L lucigenin) with a multilabel counter (Victor³ Wallac). The light signal was monitored for 5 seconds, and counts per second (CPS) were presented as NADH oxidase activity that was inhibitable by diphenyliodinium (10 µM).

Telemetry

Animals were anesthetized and a small telemetric biopotential transmitter (EA-F20, Data Sciences International, St. Paul, MN) was implanted into the abdomen. Leads (cathodal and anodal) were placed subcutaneously in a standard lead I position and sutured on each side of the chest wall. A receiver (RMC-1) was placed under the cage of each animal and connected to the data acquisition system (Dataquest A.R.T, Data Sciences International) for off-line analysis. After a 2-day period during which mice were allowed to adapt to the presence of the transmitter, mice were subjected to MI and ECG was measured over a 10-day period.

ECG Analysis

Ventricular arrhythmias were analyzed offline according to the Lambeth Convention guidelines for the analysis of experimental arrhythmias⁴. Ventricular premature beats (VPBs) were defined as singlet or doublet premature QRS complexes in relation to the P wave. Ventricular tachycardia (VT) was defined as a run of three or more premature QRS complexes and ventricular fibrillation (VF) was defined as conversion from a clear sinus rhythm without major artifact to a signal for which individual QRS complexes could no longer be distinguished from one another, usually following a clear brief period of tachycardia. For analysis of telemetric data, ECG was evaluated from 05:00-06:00, 09:00-10:00, 17:00-18:00, and 21:00-22:00 recordings from each day. All ventricular arrhythmias were expressed as the number of events (singlets, doublets and VT) per hour. The incidence and duration of VF were noted in the hour preceding death. For analysis of I/R-induced arrhythmias, the number of singlet and doublet VPBs, and the incidence and duration of VT were quantified.

Adult Cardiomyocyte Isolation

Cardiomyocytes were isolated from the hearts of adult WT and nNOS^{-/-} mice. Hearts were mounted on a Langendorff apparatus and perfused with digestion buffer containing 45 µg/mL of liberase blendzyme IV (Roche). Following digestion, cells were re-suspended and exposed to a series of sedimentation and resuspension steps in buffer containing increasing concentrations of Ca²⁺ (12.5 µM-1.0 mM). Healthy, rod-shaped myocytes were used for subsequent experiments.

Intracellular Ca²⁺ Transients

Free intracellular Ca²⁺ concentrations ([Ca²⁺]_i) were measured in isolated ventricular cardiomyocytes using fura-2-AM as previously described ⁵ with modifications. Cells were loaded with 1 μM fura-2-AM and placed into a perfusion chamber at room temperature. The chamber was placed on an inverted microscope (Nikon, Melville, NY) and perfused continuously at approximately 2 mL/min in a buffer containing (in mM) 120 NaCl, 5.4 KCl, 1.2 MgSO₄, 1.2 NaH₂PO₄, 20 NaHCO₃, and 5.6 glucose at pH 7.4. Cells were then paced at twice diastolic threshold voltage at a frequency of 0.5-4.0 Hz using a 2.5 ms duration pulse. Fluorescence intensity at 510 nm was measured using a Deltascan monochromometer system (Photon Technology International, London, ON). [Ca²⁺]_i was determined from the ratio of recorded fluorescence intensity with 340/380 nm excitation by the methods of Gryniewicz ⁶

L-Type Ca²⁺ Current

Whole-cell L-type Ca²⁺ currents were measured as described previously ⁷ with modifications. The extracellular saline solution contained (in mM) 130 NaCl, 5 KCl, 20 Hepes, 10 Glucose, 2 CaCl₂, 1 MgCl₂, with pH adjusted to 7.4 with NaOH. The pipette solution contained (in mM) 135 CsCl, 20 Hepes, 1 MgCl₂, 10 TEACl, 0.1 EGTA (pH 7.2). Ca²⁺ channel current was recorded using nystatin (300 μg/ml) perforated whole cell patch-clamp configuration. Cell capacitance was determined for each cell by applying a 10 mV hyperpolarizing pulse from the holding potential of -40 mV and integrating the resulting current trace. Currents were normalized to cell capacitance (pA/pF) to account for differences in cell size.

References

1. Feng Q, Lu X, Jones DL, Shen J, Arnold JM. Increased inducible nitric oxide synthase expression contributes to myocardial dysfunction and higher mortality after myocardial infarction in mice. *Circulation*. 2001;104:700-4.
2. Lu X, Hamilton JA, Shen J, Pang T, Jones DL, Potter RF, Arnold JM, Feng Q. Role of tumor necrosis factor-alpha in myocardial dysfunction and apoptosis during hindlimb ischemia and reperfusion. *Crit Care Med*. 2006;34:484-91.
3. Burger D, Lei M, Geoghegan-Morphet N, Lu X, Xenocostas A, Feng Q. Erythropoietin protects cardiomyocytes from apoptosis via up-regulation of endothelial nitric oxide synthase. *Cardiovasc Res*. 2006;72:51-9.
4. Walker MJ, Curtis MJ, Hearse DJ, Campbell RW, Janse MJ, Yellon DM, Cobbe SM, Coker SJ, Harness JB, Harron DW, et al. The Lambeth Conventions: guidelines for the study of arrhythmias in ischaemia infarction, and reperfusion. *Cardiovasc Res*. 1988;22:447-55.
5. Geoghegan-Morphet N, Burger D, Lu X, Sathish V, Peng T, Sims SM, Feng Q. Role of neuronal nitric oxide synthase in lipopolysaccharide-induced tumor necrosis factor-alpha expression in neonatal mouse cardiomyocytes. *Cardiovasc Res*. 2007;75:408-16.
6. Grynkiewicz G, Poenie M, Tsien RY. A new generation of Ca^{2+} indicators with greatly improved fluorescence properties. *J Biol Chem*. 1985;260:3440-50.
7. Sims SM. Calcium and potassium currents in canine gastric smooth muscle cells. *Am J Physiol*. 1992;262:G859-67.